Dissipative lattice model with exact traveling discrete kink-soliton solutions: Discrete breather generation and reaction diffusion regime

J. C. Comte,[1] P. Marquié,[1] and M. Remoissenet[2]

[1]*Laboratoire d'Electronique, Informatique et Image (LE21) Université de Bourgogne, Aile des Sciences de l'Ingénieur, BP 47870, 21078 Dijon Cedex, France*

[2]*Laboratoire de Physique de L'Université de Bourgogne (LPUB), Faculté des Sciences Mirande, 21011 Dijon, France*

(Received 7 June 1999)

We introduce a nonlinear Klein-Gordon lattice model with specific double-well on-site potential, additional constant external force and dissipation terms, which admits exact discrete kink or traveling wave fronts solutions. In the nondissipative or conservative regime, our numerical simulations show that narrow kinks can propagate freely, and reveal that static or moving discrete breathers, with a finite but long lifetime, can emerge from kink-antikink collisions. In the general dissipative regime, the lifetime of these breathers depends on the importance of the dissipative effects. In the overdamped or diffusive regime, the general equation of motion reduces to a discrete reaction diffusion equation; our simulations show that, for a given potential shape, discrete wave fronts can travel without experiencing any propagation failure but their collisions are inelastic. [S1063-651X(99)16811-9]

PACS number(s): 45.05.+x, 05.45.Yv, 63.20.Pw

I. INTRODUCTION

In recent years, the dynamics of kinks in nondissipative (Klein-Gordon) systems (for a recent review see Braun and Kivshar [1]) or traveling wave fronts in strongly dissipative or reaction diffusion systems has attracted considerable attention. It has become clear that continuous propagation equations and reaction diffusion equations provide an inadequate description of the behavior of weakly coupled lattices where the interplay between nonlinearity and spatial discreteness can lead to novel effects not present in the continuum models. For example, in nondissipative (or weakly) lattices such as: ferromagnetic chains [2], hydrogen bonded chains [3], or chain of base pairs in DNA [4], kink solitons or domain walls, whose width is of the order of few lattice spacings, may pin on the lattice owing to discreteness effects. On the other hand, in strongly dissipative lattices of coupled excitable cells, which are used as models in neurophysiology [5,6] and cardiophysiology [7] in order to describe wave propagation in nerve cells, wave propagation failure, which also originates from lattice discreteness effects [8] is an important phenomenon which may often lead to breakdown of these systems with potentially fatal consequences.

In order to gain understanding of wave motions in discrete systems, for which exact results are scarce even in one dimension, it is desirable to investigate lattice models with exact solutions. In this regard, Schmidt [9] pointed out that if the double-well on-site potential of the ϕ^4 lattice model is suitably modified, the single kink soliton becomes an exact solution to the discrete model; later, this model was shown to be integrable in the static limit and admit exact static solutions into the form of generally unpinned soliton lattices (Jensen *et al.* [10]). On the other hand, Bressloff and Rowlands [11], using an approach which presents some similarities with Jensen *et al.* [10], have recently shown that it is possible to construct exact traveling wave solutions of a discrete reaction diffusion equation, describing a system of coupled bistable elements, if the form of the bistable potential is adequately chosen. In fact, their potential corresponds precisely to Schmidt's potential. Very recently, the general problem of finding kink or pulse shaped traveling waves solutions was considered by Flach and coworkers [12]. As have the above-mentioned authors, they have approached the traveling wave existence problem from the inverse side, that is, they have shown that for a given wave problem, corresponding equations of motion can be generated, so that these equations yield the chosen wave profile as a solution. They have studied conservative lattice models and dissipative (reaction diffusion like) models, separately. One might therefore wonder if it is possible, in a similar way, to construct a general discrete model including both inertia and dissipation. Actually, generalizing Schmidt's approach, we show in this paper, that a lattice model with on-site double-well potential, with additional external force and dissipation terms, can also admit exact kink or traveling wave front solutions in any regime: nondissipative or dissipative.

The paper is organized as follows. First, we present our specific lattice model and show analytically that it can admit exact discrete kink solutions if the double-well on-site potential is adequately chosen. Then, in Sec. III, we study numerically the propagation and collisions of discrete kinks and antikinks, in the nondissipative and dissipative regimes. In Sec. IV, we consider the reaction diffusion regime and investigate numerically the properties of traveling discrete wavefronts solutions. Section V is devoted to concluding remarks.

II. MODEL AND EQUATION OF MOTION

We consider a chain of harmonically coupled particles of mass m, lying in a double well on site potential U. This system is modeled by the general discrete equation of motion

$$m\frac{d^2u_n}{dt^2}+\Gamma\frac{du_n}{dt}=k[u_{n+1}-2u_n+u_{n-1}]-F-\frac{dU(u_n)}{du_n}, \quad (2.1)$$

where u_n is the nth particle displacement, Γ is a dissipative coefficient, and k is a coupling term. F is a constant term which may be an external force and the energy gain due to F is compensated by the loss mechanism. We assume that a traveling wave front solution of (2.1) has the following kink shape:

$$u_n(t)=u_0\tanh(\omega t-\kappa na). \quad (2.2)$$

Here, u_0 is the amplitude, a the lattice spacing, and ω and κ are two constants such that the ratio $c=\omega/\kappa$ represents the velocity of the front. Following Schmidt [9], we construct a potential, including the external potential, which has the form:

$$V(u_n)=Fu_n+U(u_n)$$
$$=Fu_n-A\frac{u_n^2}{2}+B_0\frac{u_n^3}{3}+B\frac{u_n^4}{4}+C_0\frac{u_n^5}{5}+C\frac{u_n^6}{6}+D_0\frac{u_n^7}{7}$$
$$+D\frac{u_n^8}{8}+\cdots, \quad (2.3)$$

such that the expression (2.2) becomes an exact discrete solution of (2.1). Here, A,B_0,B,C_0,C,D_0,D, represent constant coefficients. The detailed calculations are presented in the Appendix. We obtain the new equation of motion

$$\frac{m}{k}\frac{d^2v_n}{dt^2}+\frac{\Gamma}{k}\frac{dv_n}{dt}=-\frac{dV(v_n)}{dv_n}+[v_{n+1}-2v_n+v_{n-1}], \quad (2.4)$$

where we have introduced the dimensionless variable $v_n=\tau(u_n/u_0)$, with $\tau=\tanh(\kappa a)$. Here $V(v_n)$ is given by

$$V(v_n)=\alpha v_n+\beta v_n^2+\gamma v_n^3+\delta v_n^4+\xi\ln(1-v_n^2), \quad (2.5)$$

with $\alpha=-\Gamma\omega\tau/k$, $\beta=(m\omega^2/k-1)$, $\gamma=\Gamma\omega/(k\tau)$, $\delta=-m\omega^2/(2k\tau^2)$, and $\xi=-2(\tau^2-1)$. The propagation velocity of the front is given by

$$c=\frac{\omega}{\kappa}=\frac{a\omega}{\operatorname{arctanh}(\tau)}. \quad (2.6)$$

The general discrete equation of motion (2.4) with potential (2.5) and solution

$$v_n=\tau\tanh(\omega t-\kappa na), \quad (2.7)$$

is valid for any value of F and Γ. At this stage, three different cases can be considered.

(i) When $m\neq 0$ and $\Gamma=0$, the coefficients of v_n and v_n^3 in (2.5) become zero, the symmetry breaking due to F disappears and the potential becomes symmetric with two degenerate minima. One recovers the conservative system studied by Schmidt [9]; the total energy is constant and to each (ω, κ) combination corresponds a different well shape and velocity.

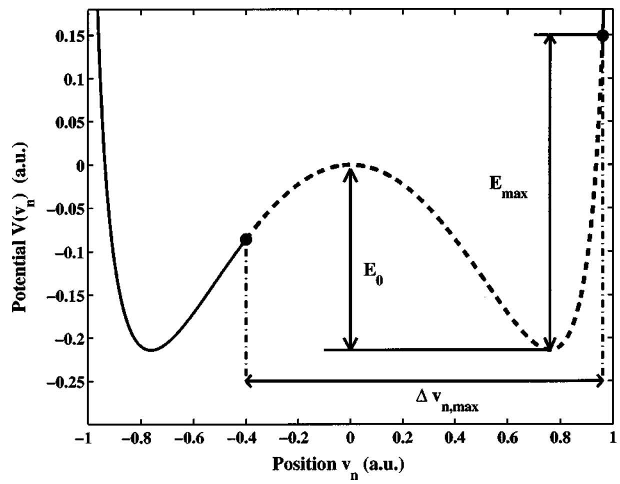

FIG. 1. Symmetric potential $V(v_n)$ in the nondissipative regime with its two degenerate minima. The shape is obtained with the parameters $\omega=0.0493$ and $\tau=0.761$. The dashed line represents the asymmetric oscillations of the central particles of the breather (with an amplitude $\Delta v_{n,\max}=1.36$) created by the kink-anti-kink collision. $E_{\max}$ represents the maximum of energy of the particles during the oscillations while E_0 is the energy barrier height.

(ii) When $m\neq 0$, $\Gamma\neq 0$, this is the general case where both inertial and dissipative effects play a role. The value of ω is imposed [see Eq. (A7)] by the relation $F=-\omega u_0\Gamma$. It turns out that the potential well shape and velocity both depend uniquely on the choice of κ, that is τ.

(iii) When $\Gamma\neq 0$ and $m=0$, the lattice dynamics becomes overdamped or diffusive. In (2.5), β, the coefficient of v_n^2 reduces to -1 and δ, the coefficient of v_n^4 becomes zero: the potential is asymmetric with two nondegenerate minima. This regime corresponds to the model studied by Bressloff and Rowlands [11].

In the following we consider these three cases successively.

III. NONDISSIPATIVE AND DISSIPATIVE REGIMES

A. Nondissipative regime

In this case $(\Gamma=0)$, the potential, represented in Fig. 1, becomes

$$V(v_n)=\left(m\frac{\omega^2}{k}-1\right)v_n^2-m\frac{\omega^2}{2k\tau^2}v_n^4-2(\tau^2-1)\ln(1-v_n^2). \quad (3.1)$$

The barrier height is given by (3.2),

$$E_0=\left|\tau^2\left(1-\frac{\omega^2}{2\omega_0^2}\right)-(1-\tau^2)\ln(1-\tau^2)\right|, \quad (3.2)$$

with $\omega_0^2=k/m$. The equation of motion (2.4) is written as

$$\frac{d^2v_n}{dt^2}=\omega_0^2[v_{n+1}-2v_n+v_{n-1}]$$
$$+\omega_0^2\left[\frac{2\omega^2}{\omega_0^2\tau^2}v_n(v_n^2-\tau^2)+2v_n-2(1-\tau^2)\frac{v_n}{1-v_n^2}\right]. \quad (3.3)$$

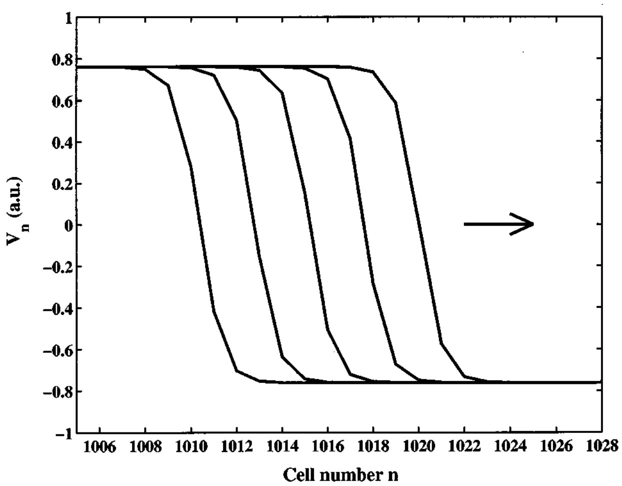

FIG. 2. Traveling kink K with a width of five lattice spacings and a constant velocity $c = 0.023\ \mathrm{cell\,s^{-1}}$ in the nondissipative regime.

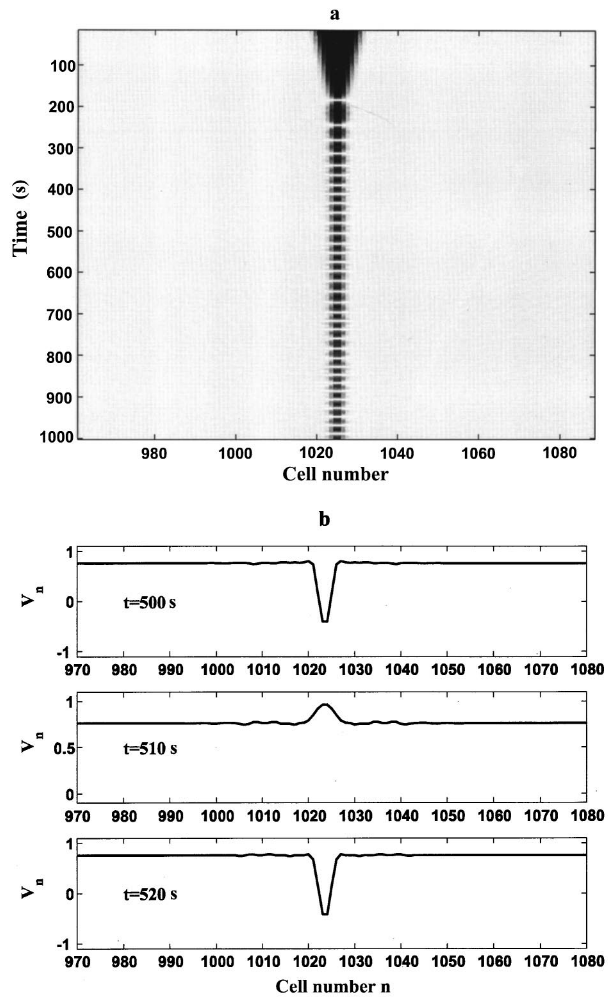

FIG. 3. (a) Creation of a discrete stationary breather with a small amplitude radiation background by a $K-\overline{K}$ collision. (b) Representation of the breather at three different times ($t = 500$ s, $t = 510$ s, and $t = 520$ s) allowing to observe its behavior over one period of oscillation $T_B = 20$ s: the oscillations of the central particle are asymmetric with an amplitude $\Delta v_{n,\max} = 1.36$ (see Fig. 1).

We have checked by numerical simulations that an exact discrete kink solution given by (2.7) can propagate freely, that is, without experiencing any discreteness effect. In Fig. 2, we have represented, at different times, a kink K with a width of five lattice spacings traveling in a lattice of 2048 cells. The parameters of the lattice and the potential are, respectively, $k = 0.1$ and $m = 1$, $\omega = 0.0493$ and $\tau = 0.761$. Under these conditions, the velocity of the kink is $c = 0.023\ \mathrm{cell\,s^{-1}}$. Note that no radiation effects are observed which confirms that (2.7) is an exact solution.

Then we have studied the possible generation of nonlinear localized modes or discrete breathers via kink (K) and antikink ($\overline{K}$) collisions. This investigation was motivated by the interesting properties of discrete breathers: these nontopological excitations can exist in a large variety of nonlinear lattices and their existence is associated with a localization of energy (for recent reviews see [13,14]). Specifically, we have studied numerically a $K-\overline{K}$ collision where the two entities travel at velocity $c = 0.023\ \mathrm{cell\,s^{-1}}$ and $-c$, respectively. As shown in Fig. 3(a), a discrete stationary breather and a small amplitude radiation background emerge from the weakly inelastic $K-\overline{K}$ collision. In Fig. 3(b), we have represented this breather at three different times, $t = 500$ s, $t = 510$ s, and $t = 520$ s, respectively, such that we can observe its behavior over one period T_B of oscillation: $T_B = 20$ s. The oscillations of the central particules of the breather are asymmetric with an amplitude $\Delta V_{n,\max} = 0.96 + |-0.4| = 1.36$, as represented by the dashed line in Fig. 1. Indeed, during the oscillations from $E_{\max} = 0.364$ to $E = -0.086$, the central particles overcome the potential barrier $E_0 = |-0.214|$, given by (3.2). In the breather spectrum, the fundamental angular frequency $\omega_B = 2\pi/T_B = 0.314\ \mathrm{rad\,s^{-1}}$ is represented by a in Fig. 4, while the second and third harmonics are, respectively, represented by b and c. Although the breather looks like very stable, it radiates phonons very slowly. The radiation frequency corresponds to the third harmonics in the breather spectrum (c in Fig. 4) which actually represents only 2% of the energy of the first harmonic. Specifically, the frequency of this third harmonic lies in the phonon band given by $\omega = \omega_0 \sqrt{2[(1-\lambda) - \cos(\kappa a)]}$, as shown in Fig. 4, where $\lambda = 1 - 2(\omega^2/\omega_0^2) - (1+\tau^2)/(1-\tau^2)$. As a result, this small radiation can propagate. Nevertheless, in spite of these weak radiation losses, this discrete breather has an important lifetime and presents a physical interest. We have also investigated the collision of a static kink ($c = 0$) with a kink moving at velocity $c = 0.023\ \mathrm{cell\,s^{-1}}$. Such a collision results in a discrete breather with the same properties as the static one, but moving at mean velocity $c_b = 0.013\ \mathrm{cell\,s^{-1}}$.

B. General dissipative regime

In the general regime, where both inertial and dissipative terms are present, we have analyzed numerically a $K-\overline{K}$ collision. As pointed out in Sec. II, the potential well shape and velocity both depend on the choice of τ. In this case, as it should be expected, we have observed that the number N of breathing oscillations depends on Γ/m. For example, we have the following results: $N = 27$ for $\Gamma/m = 0.001$, $N = 8$ for $\Gamma/m = 0.01$, and $N = 2$ for $\Gamma/m = 0.1$. For $\Gamma/m > 0.1$, the number of oscillations decreases and tends rapidly to zero. Our results suggest that in real lattices, where dissipation

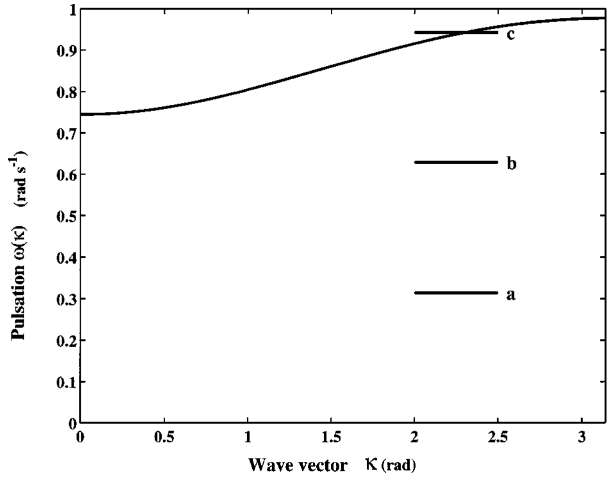

FIG. 4. Breather spectrum: the fundamental angular frequency $\omega_B = 0.314$ rad s^{-1} is represented by letter *a* while the second and third harmonics are respectively represented by *b* and *c*. The third harmonics (*c*) lies in the phonon band (represented by the continuous line) leading to small radiations of the breather.

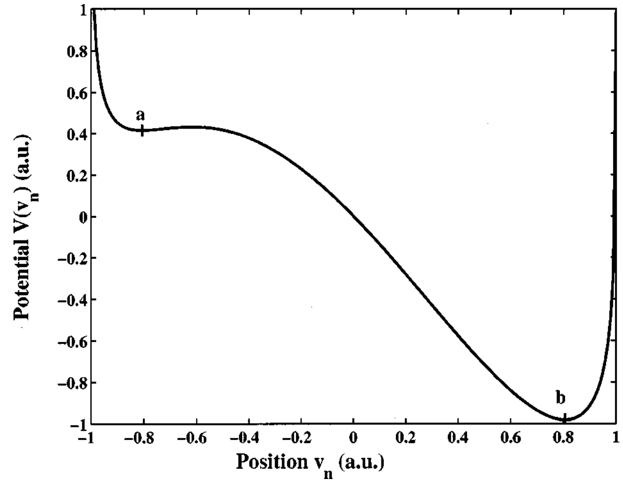

FIG. 5. Asymmetric potential $V(v_n)$ in the strongly dissipative or diffusive regime. Letters *a* and *b* represent the two nondegenerate minima.

cannot be ignored, the existence of breathers is relevant only in the case of weak dissipation. Actually, this general regime, which should present unexpected features for some parameters range, remains to be explored carefully and will be discussed elsewhere.

IV. STRONGLY DISSIPATIVE OR DIFFUSIVE REGIME

Let us now focus on the overdamped or diffusive case $(m=0)$. Equation (2.4) then reduces to

$$\Gamma \frac{dv_n}{dt} = k[v_{n+1} - 2v_n + v_{n-1}] + \left[\Gamma\omega\tau + 2kv_n - \frac{\Gamma\omega}{\tau} v_n^2 + 2k(\tau^2 - 1)\frac{v_n}{1-v_n^2}\right]. \tag{4.1}$$

In order to compare our results (see hereafter) to those of Bressloff and Rowlands [11], we perform the following transformations. We divide the two members of (4.1) by Γ and set $D = k/\Gamma$, $\varepsilon_D = \omega/(\tau D)$ and $\alpha_0 = 2(1-\tau^2)$, to obtain

$$\frac{dv_n}{dt} = D[v_{n+1} - 2v_n + v_{n-1}] + D\left[\varepsilon_D[(1-\alpha_0/2) - v_n^2] - \frac{\alpha_0 v_n}{1-v_n^2} + 2v_n\right]. \tag{4.2}$$

Equation (4.2) is a discrete reaction diffusion [7] equation of the form:

$$\frac{dv_n}{dt} = D[v_{n+1} - 2v_n + v_{n-1}] + f(v_n), \tag{4.3}$$

with kink-shaped solution (2.7) provided that, the potential $V(v_n)$ is well chosen. Indeed, the potential corresponding to $f(v_n)$ is

$$V(v_n) = D\left[\varepsilon_D(1-\alpha_0/2)v_n + v_n^2 - \varepsilon_D \frac{v_n^3}{3} + (\alpha_0/2)\ln(1-v_n^2)\right]. \tag{4.4}$$

Note that, for $D=1$, relation (4.3) is identical to the equation (1.3) of Bressloff and Rowlands in [11]. The potential (4.4), represented in Fig. 5 as a function of v_n, is asymmetric with two nondegenerate minima (*a* and *b* in Fig. 5). The value of ω is imposed by F and the velocity of the discrete front solution of (4.2) depends on the choice of $\tau = \tanh(\kappa a)$. The velocity of the front expressed in terms of the new parameters α_0 and ε_D is

$$c = \omega/\kappa = \frac{\varepsilon_D D}{\tau} = \frac{\varepsilon_D D}{\sqrt{1-\alpha_0/2}}. \tag{4.5}$$

This velocity c is proportional to the diffusion coefficient D, as represented in Fig. 6 by the continuous linear curves (obtained for different values of coefficient α). In this figure are also superimposed the results obtained by numerical simulations. They have been performed on a lattice of 2048 particles, for different values of the diffusion coefficient D and the α_0 coefficient. The initial condition consists in a front given by relation (2.7). One can observe that the velocities measured during the simulations (plus signs in Fig. 6) are very well fitted by the theoretical curves. The fundamental result, in the diffusive case, is the nonexistence of propagation failure, contrary to the systems described by a discrete reaction diffusion equation of the Fitzhugh-Nagumo type [8,15,16]. Indeed, in these systems, there exists a critical value of the coupling constant (or the diffusion coefficient) under which propagation of diffusion of fronts becomes impossible [15]. Considering the discrete lattice with the potential given by relation (4.4), we observe numerically that, for any value of the diffusion coefficient D (except for $D=0$ when all the particles are independent), there exists a traveling wave front. In fact, for a lattice with a given coupling constant, we have constructed a potential for which a propa-

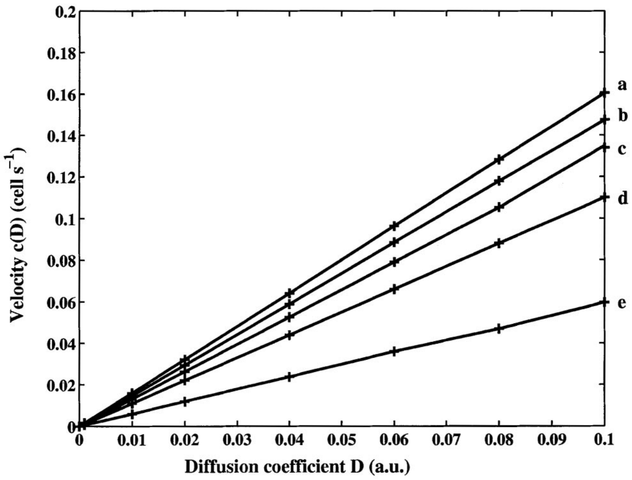

FIG. 6. Theoretical velocity of the front [Eq. (4.5)] in the diffusive case for different values of the parameter α (continuous lines): (a) $\alpha=1$; (b) $\alpha=0.75$; (c) $\alpha=0.5$; (d) $\alpha=0.25$; (e) $\alpha=0.01$. The measured velocity during simulations (+ signs) are very well fitted by theoretical curves given by Eq. (4.5).

gative discrete solution of the form (2.7) exists. But if we modify the coupling constant of this lattice without changing the potential shape, then expression (2.7) is no more a solution of the reaction diffusion equation (4.2). As a result, in this case, we find that propagation failure occurs, as shown also by Bressloff and Rowlands [11]. We have then observed that the collision between two wave fronts traveling in opposite directions results into their annihilation.

V. CONCLUDING REMARKS

The generalized dissipative nonlinear Klein-Gordon lattice model that we have introduced, interpolates between the Schmidt's model [9] in the conservative regime and the reaction diffusion model of Bressloff and Rowlands [11] in the overdamped regime. Like Flach and coworkers [12] we have used an inverse method. However, contrary to these authors who have considered the conservative and dissipative lattice models separately, we have investigated a lattice model which includes *both* inertia and dissipation, like many systems in the real world. We have shown analytically that our lattice equations admit exact discrete kink or traveling wave fronts solutions if the double-well on-site potential is adequately chosen. In the nondissipative regime, we have checked numerically that discrete kink (antikink) solutions can propagate freely without experiencing any discreteness effects. Kink-antikink collisions reveal that static or moving discrete breathers with finite but with physically interesting lifetimes can be generated. In the general dissipative regime, discrete kinks can propagate freely and the lifetimes of the discrete breathers that can be created by collisions between these kinks depend on the importance of the dissipation. These results are interesting: they suggest that, for the real lattices where dissipation cannot be ignored, discrete kinks can travel and combine to generate discrete breathers with reasonable lifetimes, if dissipative effects are weak enough compared to inertial effects. In the overdamped or diffusive regime, discrete kinks or wave fronts can travel without experiencing any lattice effects or propagation failure. However, in this case, their collisions are totally inelastic. We would like to point out again that our model and results are relevant for physical systems in which the discreteness of the lattice is important. Obviously, further studies are necessary in the general dissipative regime to determine all the properties of these kinks with exceptional mobilities. In conclusion, we believe that the understanding of discrete nonlinear models is an active and attractive topic of the current research. Since realistic physical models are rather complicated, it is extremely important to develop the basic concepts with the help of simple lattice models with exact solutions.

APPENDIX: CALCULATIONS DETAILS

Starting from (2.1), we seek a total potential $V(u_n)=Fu_n+U(u_n)$ under the form (2.3) such that (2.2) is an exact solution of (2.1). Setting $T_n=\tanh(\omega t-\kappa na)$ and $\tau=\tanh(\kappa a)$ we then get

$$\frac{du_n}{dt}=u_0(1-T_n^2)\omega, \tag{A1}$$

$$\frac{d^2u_n}{dt^2}=-2u_0\omega^2(1-T_n^2)T_n\,, \tag{A2}$$

$$u_{n+1}+u_{n-1}=u_0[\tanh[\omega t-\kappa(n+1)a]+\tanh[\omega t-\kappa(n-1)a]]=2u_0(1-\tau^2)T_n(1+\tau^2T_n^2+\tau^4T_n^4+\cdots), \tag{A3}$$

and

$$\frac{dV(u_n)}{du_n}=F-Au_n+B_0u_n^2+Bu_n^3+C_0u_n^4+Cu_n^5+D_0u_n^6+Du_n^7+\dots\,. \tag{A4}$$

Substituting relations (A1), (A2), and (A3) in (2.1) yields

$$-2mu_0\omega^2T_n(1-T_n^2)+\Gamma\omega u_0(1-T_n^2)-2u_0k(1-\tau^2)T_n(1+\tau^2Tn^2+\tau^4T_n^4+\cdots)+2ku_0T_n+F-Au_0T_n+B_0u_0^2T_n^2+Bu_0^3T_n^3$$
$$+C_0u_0^4T_n^4+Cu_0^5T_n^5+Du_0^6T_n^6+Du_0^7T_n^7+\cdots=0. \tag{A5}$$

Writing this equation as a power series in T_n, we get

$$(F+\Gamma\omega u_0)+T_n[2ku_0-Au_0-2mu_0\omega^2-2ku_0(1-\tau^2)]+T_n^2(B_0u_0^2-\gamma\omega u_0)+T_n^3[2mu_0\omega^2-2ku_0(1-\tau^2)\tau^2+Bu_0^3]$$
$$+T_n^4C_0u_0^4+T_n^5[Cu_0^5-2u_0k(1-\tau^2)\tau^4]+T_n^6D_0u_0^6+T_n^7[Du_0^7-2ku_0(1-\tau^2)\tau^6]+\cdots=0. \tag{A6}$$

Equation (A6) is satisfied for all t and all n, if each coefficient of the series vanishes, yielding:

$$F=-\Gamma\omega u_0,\quad C_0=0,$$
$$A=2(k\tau^2-m\omega^2),\quad C=\frac{2}{u_0}[k\tau^4(1-\tau^2)],$$
$$B_0=\frac{\Gamma\omega}{u_0},\quad D_0=0, \tag{A7}$$
$$B=\frac{2}{u_0^2}[k\tau^2(1-\tau^2)-m\omega^2],\quad D=\frac{2}{u_0^6}k\tau^6(1-\tau^2).$$

The potential expression becomes

$$V(u_n)=ku_0^2\left[-\frac{\Gamma\omega}{k}\frac{u_n}{u_0}+\left(\frac{m\omega^2}{k}-1\right)\frac{u_n^2}{u_0^2}+\frac{\Gamma\omega}{3k}\frac{u_n^3}{u_0^3}-\frac{m\omega^2}{2k}\frac{u_n^4}{u_0^4}+\frac{1-\tau^2}{\tau^2}\left(\tau^2\frac{u_n^2}{u_0^2}+\frac{\tau^4}{2}\frac{u_n^4}{u_0^4}+\frac{\tau^6}{3}\frac{u_n^6}{u_0^6}+\frac{\tau^8}{4}\frac{u_n^8}{u_0^8}+\cdots\right)\right]. \tag{A8}$$

Then (A8) can be rearranged to give

$$V(u_n)=ku_0^2\left[-\frac{\Gamma\omega}{k}\left(\frac{u_n}{u_0}\right)+\left(\frac{m\omega^2}{k}-1\right)\left(\frac{u_n}{u_0}\right)^2+\frac{\Gamma\omega}{3k}\left(\frac{u_n}{u_0}\right)^3-\frac{m\omega^2}{2k}\left(\frac{u_n}{u_0}\right)^4+\left(1-\frac{1}{\tau^2}\right)\ln\left[1-\tau^2\left(\frac{u_n}{u_0}\right)^2\right]\right]. \tag{A9}$$

Equation (2.1) then becomes

$$m\frac{d^2u_n}{dt^2}+\Gamma\frac{du_n}{dt}=k[u_{n+1}-2u_n+u_{n-1}]-ku_0\left[-\frac{\Gamma\omega}{k}+2\left(\frac{m\omega^2}{k}\right)\frac{u_n}{u_0}+3\frac{\Gamma\omega}{3k}\frac{u_n^2}{u_0^2}-4\frac{m\omega^2}{2k}\frac{u_n^3}{u_0^3}+\left(1-\frac{1}{\tau^2}\right)\frac{-2\tau^2\frac{u_n}{u_0}}{1-\tau^2\frac{u_n^2}{u_0^2}}\right]. \tag{A10}$$

Finally, setting $v_n=\tau(u_n/u_0)$ and $\tau=\tanh(\kappa a)$, we obtain the general dimensionless equation of motion,

$$m\frac{d^2v_n}{dt^2}+\Gamma\frac{dv_n}{dt}=k[v_{n+1}-2v_n+v_{n-1}]-k\frac{dV(v_n)}{dt} \tag{A11}$$

which becomes

$$m\frac{d^2v_n}{dt^2}+\Gamma\frac{dv_n}{dt}=k[v_{n+1}-2v_n+v_{n-1}]-k\left[\alpha+2\beta v_n+3\gamma v_n^2+4\delta v_n^3+\xi\frac{v_n}{1-v_n^2}\right], \tag{A12}$$

with $\alpha=-\Gamma\omega\tau/k$, $\beta=(m\omega^2/k-1)$, $\gamma=\Gamma\omega/(k\tau)$, $\delta=-m\omega^2/(2k\tau^2)$, $\xi=-2(\tau^2-1)$.

[1] O. M. Braun and Y. S. Kivshar, Phys. Rep. **306**, 1 (1998).
[2] A. R. Bishop and T. F. Lewis, J. Phys. C **12**, 3811 (1979).
[3] O. M. Braun, F. Zhang, Y. S. Kivshar, and L. Vasquez, Phys. Lett. A **157**, 241 (1991).
[4] M. Peyrard and A. R. Bishop, Phys. Rev. Lett. **62**, 2755 (1989).
[5] J. Nagumo, S. Arimoto, and S. Yoshisawa, Proc. IRE **50**, 2061 (1962).
[6] A. C. Scott, Rev. Mod. Phys. **47**, 487 (1975).
[7] J. D. Murray, *Mathematical Biology* (Springer-Verlag, Berlin, 1989).
[8] J. P. Keener, SIAM (Soc. Ind. Appl. Math.) J. Appl. Math. **47**, 556 (1987).
[9] V. H. Schmidt, Phys. Rev. B **20**, 4397 (1979).
[10] M. H. Jensen, P. Bak, and A. Popielewicz, J. Phys. A **16**, 4369 (1983).
[11] P. C. Bressloff and G. Rowlands, Physica D **106**, 255 (1997).
[12] S. Flach, Y. Zolotaryuk, and K. Kladko, Phys. Rev. E **59**, 6105 (1999).
[13] S. Aubry, Physica D **103**, 201 (1997).
[14] S. Flach and C. R. Willis, Phys. Rep. **295**, 181 (1998).
[15] T. Erneux and G. Nicolis, Physica D **67**, 237 (1993).
[16] V. Perez-Munuzuri, V. Perez-Villar, and L. O. Chua, Journal Circuits, Syst. Comput. **3**, 215 (1993).